ADVANCED FUNCTIONAL MATERIALS
www.afm-journal.de

Pyrolyzed Cobalt Corrole as a Potential Non-Precious Catalyst for Fuel Cells

Hsin-Chih Huang, Indrajit Shown, Sun-Tang Chang, Hsin-Cheng Hsu, He-Yun Du, Ming-Cheng Kuo, Ken-Tsung Wong, Sea-Fu Wang, Chen-Hao Wang, Li-Chyong Chen, and Kuei-Hsien Chen**

Non-precious metal catalysts of the oxygen reduction reaction are highly favored for use in polymer electrolyte fuel cells (PEFC) because of their relatively low cost. Here, a new carbon-black-supported pyrolyzed Co-corrole (py-Co-corrole/C) catalyst of the oxygen reduction reaction (ORR) in a PEFC cathode is demonstrated to have high catalytic performance. The py-Co-corrole/C at 700 °C exhibits optimized ORR activity and participates in a direct four-electron reduction pathway for the reduction of O_2 to H_2O. The H_2-O_2 PEFC test of py-Co-corrole/C in the cathode reveals a maximum power density of 275 mW cm^{-2}, which yields a higher performance and a lower Co loading than previous studies of Co-based catalysts for PEFCs. The enhancement of the ORR activity of py-Co-corrole/C is attributable to the four-coordinated Co-corrole structure and the oxidation state of the central cobalt.

1. Introduction

A polymer electrolyte fuel cell (PEFC) is an electrochemical device that transforms chemical energy to electrical energy by the redox reaction of hydrogen and air (oxygen), which are fed into the anode and the cathode, respectively. The core unit of the PEFC, a membrane-electrode-assembly (MEA), is composed of a polymer electrolyte membrane that is sandwiched between an anode and a cathode, both of which contain precious catalysts i.e., platinum. The oxygen reduction reaction (ORR) in the cathode is much slower than the hydrogen oxidation reaction in the anode,[1] and therefore, to accelerate the ORR, a high loading of platinum (Pt) catalyst is used in the cathode, making the PEFC expensive. The high price associated with use of an extremely rare earth Pt catalyst in fuel cells is the factor that mostly limits their commercialization. Unconventional non-platinum catalysts, which are efficient, durable and inexpensive, must be developed to replace Pt catalysts in the ORR.

Since Jasinski investigated cobalt phthalocyanine as a catalyst of the reaction at the cathode in a fuel cell in 1964,[2] various studies have demonstrated that macrocyclic complexes with transition metal, including porphyrin,[3] phthalocyanine[4] and tetraazannulene[5] are candidate catalysts of ORR. Among those, iron and cobalt-based macrocyclic compounds have been claimed to have the highest catalytic activity in the ORR.[6] In 2006, Bashyam et al. were the first to demonstrate the use of non-precious metal composite (cobalt-polypyrrole) catalysts in the cathode of a H_2-O_2 PEFC at 80 °C, with a maximum power density of approximately 150 mW cm^{-2}, and no significant degradation over at least 100 hours.[7] Lefevre et al. showed that the current density of microporous carbon-supported iron-based catalysts in the ORR equals that of precious metals at a cell voltage of ≥0.9 V.[8] Recently, Wu et al. utilized polyaniline as a precursor to a carbon-nitrogen template in the high-temperature synthesis of catalysts that incorporate iron and cobalt that exhibited high activity and remarkable performance stability.[9] Proietti et al. used an iron-acetate/phenanthroline/zeolitic-imidazolate-framework-derived electrocatalyst with increased volumetric activity and enhanced mass-transport properties. The PEFCs test in H_2-O_2, has a power density of 0.75 W cm^{-2} at 0.6 V, which is the best performance of non-precious metal ORR catalyst to date.[10] Some review articles have been studied non-precious metal ORR catalyst, which transition metal nitrogen-containing complexes are considered the most promising ORR catalysts.[6c,11]

H.-C. Huang, Dr. I. Shown, Dr. H.-Y. Du, Prof. K.-H. Chen
Institute of Atomic and Molecular Science
Academia Sinica, Taipei 10617, Taiwan
E-mail: chenkh@pub.iams.sinica.edu.tw
H.-C. Huang, S.-T. Chang, H.-C. Hsu, Prof. C.-H. Wang
Department of Materials Science and Engineering
National Taiwan University of Science and Technology
Taipei 10607, Taiwan
E-mail: chwang@mail.ntust.edu.tw
H.-C. Huang, Prof. S.-F. Wang
Department of Materials and Mineral Resources Engineering
National Taipei University of Technology
Taipei 10608, Taiwan
M.-C. Kuo, Prof. K.-T. Wong
Department of Chemistry
National Taiwan University
Taipei 10617, Taiwan
Prof. L.-C. Chen
Center for Condensed Matter Sciences
National Taiwan University
Taipei 10617, Taiwan

DOI: 10.1002/adfm.201200264

The poor performance of existing non-precious metal catalysts in commercial fuel cells emphasizes the need for more research into the development of an alternative catalyst for PEFC applications.

In the past few years, the corrole chemistry has advanced considerably. The corrole has been shown to be a versatile ligand that can coordinate with transition metals without significant distortion of the macrocycle plane. The corrole is a tetrapyrrolic macrocyclic compound with one carbon atom fewer than porphyrin. The particular ligand behavior of corrole is of interest because of its catalyst application of the redox reaction.[12] The corrole acts as a trianionic ligand, unlike both corrins and porphyrins, which are monoanionic and dianionic ligands, respectively. Additionally, the ability of corrole to stabilize higher oxidation states of a metal than porphyrins makes its coordination chemistry particularly interesting.

This work elucidates a simple synthesis of pyrolyzed Co-corrole supported by carbon black (py-Co-corrole/C) use in the ORR. The py-Co-corrole/C catalyst accelerates the ORR in a fuel cell beyond the rate achieved using other cobalt-containing macrocyclic compounds, such as porphyrin, phthalocyanine, and tetraazannulene. This work is the first to report on pyrolyzed Co-corrole as a non-precious metal catalyst for use in fuel cells.

2. Results and Discussion

The ORR pathway mainly involves the following reactions.

Reaction 1: $O_2 + 4H^+ + 4e^- \rightarrow 2H_2O \quad E^0 = 1.229$ V

Reaction 2: $O_2 + 2H^+ + 2e^- \rightarrow H_2O_2 \quad E^0 = 0.695$ V

Reaction 3: $H_2O_2 + 2H^+ + 2e^- \rightarrow 2H_2O \quad E^0 = 1.763$ V

H_2O_2 may also chemically decompose into O_2 and H_2O.

Reaction 1 follows a direct reduction pathway that involves a four-electron transfer. Reaction 2 follows an H_2O_2 pathway that involves a two-electron transfer. Since a direct ORR pathway yields a higher thermodynamically reversible potential than an H_2O_2 pathway, Reaction 1 is favored over Reaction 2 as the ORR in the PEFC.

When the macrocyclic/transition metal complexes (M-N_4 moieties, M: Co and Fe) are pyrolyzed at a particular temperature, their structures are partially or completely destroyed, resulting in new active sites that have greater and more stable ORR activity than the untreated M-N_4 moieties. **Figure 1** plots the results of the TGA analysis of the pristine Co-corrole without carbon supports. The pristine Co-corrole begins to decompose at 250 °C, and is relatively stable between 300 and 750 °C. The total weight loss is 36% of the initial weight at 700 °C. According to previous investigations of CoTMPP and cobalt phthalocyanine, some of the cobalt-containing nitrogen chelate is cleaved and bound to other atoms, forming Co-N_x-C_y as a poly-aromatic graphite-like structure, increasing the electrical conductivity of catalysts.[13] To elucidate the effect of the pyrolyzed temperature, pyrolyzed Co-corrole supported by carbon black was prepared at various temperatures of 300, 500, 700 and 900 °C. The formed compounds were py-Co-corrole/C-300, py-Co-corrole/C-500, py-Co-corrole/C-700 and py-Co-corrole/C-900, respectively. **Figure 2**a presents the ORR activities of py-Co-corrole/C-300, py-Co-corrole/C-500, py-Co-corrole/C-700 and py-Co-corrole/C-900. The lower part of Figure 2a plots disk current (I_d) against applied potential and the upper part plots the ring current (I_r) as a function of applied potential. At a pyrolyzed temperature of 700 °C, the highest absolute value of I_d and the lowest absolute of I_r were. The total electron-transfer number (n) and the hydrogen peroxide yield (%H_2O_2) in the catalyzed ORR were utilized,

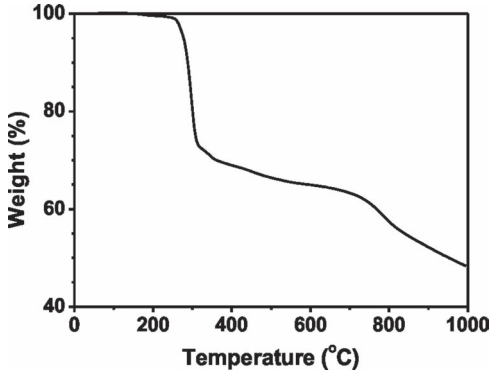

Figure 1. TGA curve of Co-corrole without carbon black. The sample was kept under a constant flux of N_2.

$$n = \frac{4 I_d}{I_d + \frac{I_r}{N}} \quad (1)$$

$$\%H_2O_2 = \frac{\frac{2 I_r}{N}}{I_d + \frac{I_r}{N}} \times 100\% \quad (2)$$

where N is the RRDE collection efficiency, which was determined to be 0.37 herein. Figure 2b,c display the n values and%H_2O_2, respectively. The observations demonstrate that the pyrolysis at 700 °C yields the highest n and the lowest% H_2O_2.

Figure 3 presents the XRD patterns of py-Co-corrole-700, pristine Co-corrole and the reference β-Co (JCPDS, PDF# 150806). XRD patterns of pristine Co-corrole included numerous characteristic peaks, but after the pyrolysis, the pattern included only three characteristic peaks at approximately 26°, 44° and 51°, which correspond to C(002), β-Co(111) and β-Co(200), respectively. The XRD peaks of crystalline cobalt reveal that part of the Co-corrole ring is somewhat decomposed to metallic cobalt during pyrolysis. Studies of other M-N_4 moieties in the ORR have yielded similar results, in which the M-N_4 moiety was partially or completely decomposed in the pyrolysis.[14] Raman spectra demonstrate py-Co-corrole-700 showing two strong peaks at 1330 and 1580 cm^{-1}, which are related to D- and G-peaks, respectively, of the carbon-like materials, as shown in Figure S1 in the Supporting Information. It suggests that py-Co-corrole-700 forms a network structure of poly-aromatic hydrocarbons.

The $Co2p_{3/2}$ XPS spectra of py-CoTMPP-700 and py-Co-corrole-700 are shown in **Figure 4** and **Figure 5**, respectively. The corresponding fitting results are shown in **Table 1**, Py-Co-corrole-700 shows that the contents of Co(0) and Co(II)O are approximately 5.3% and 94.7%, respectively. Py-CoTMPP-700 shows that the contents of Co(0), Co(II)O and Co(II)Nx are 32.7%, 43.7%, and 23.6%, respectively. **Figure 6** demonstrates XPS N1s spectra of pristine Co-corrole and py-Co-corrole-700, which the corresponding fitting results are shown in **Table 2**.

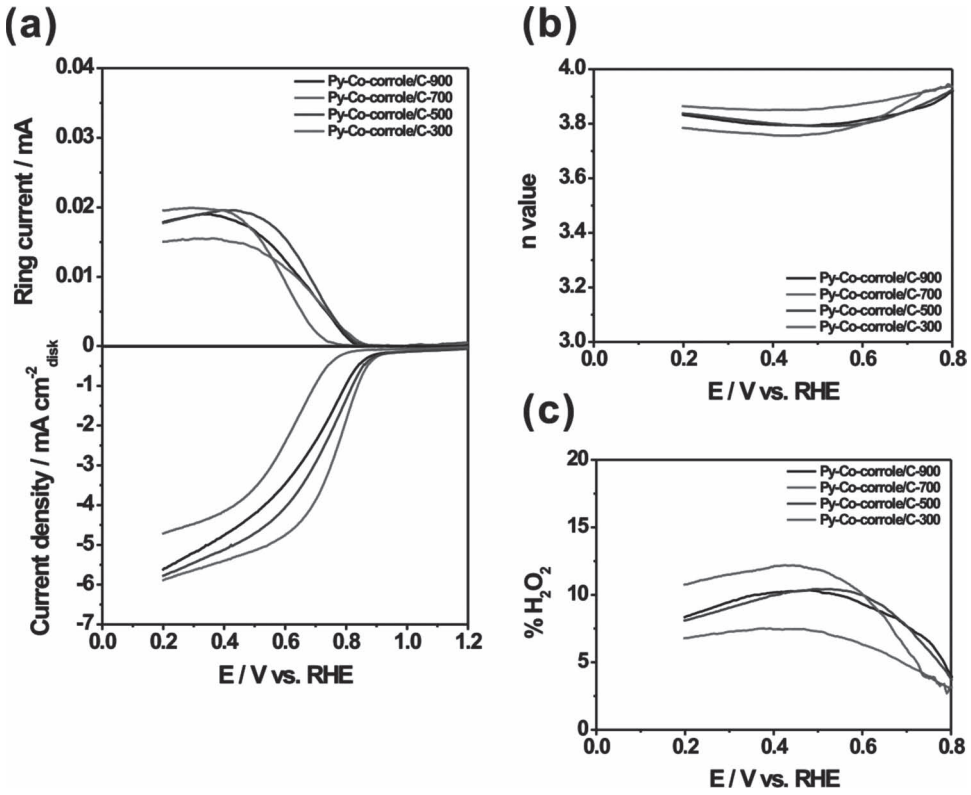

Figure 2. a) ORR curves for py-Co-corrole/C at different temperatures, b) the *n* values, and c) %H_2O_2 of the catalysts dependence on disk potentials. Rotating speed: 1600 rpm; scan rate: 10 mV s^{-1}; ring potential: 1.2 V.

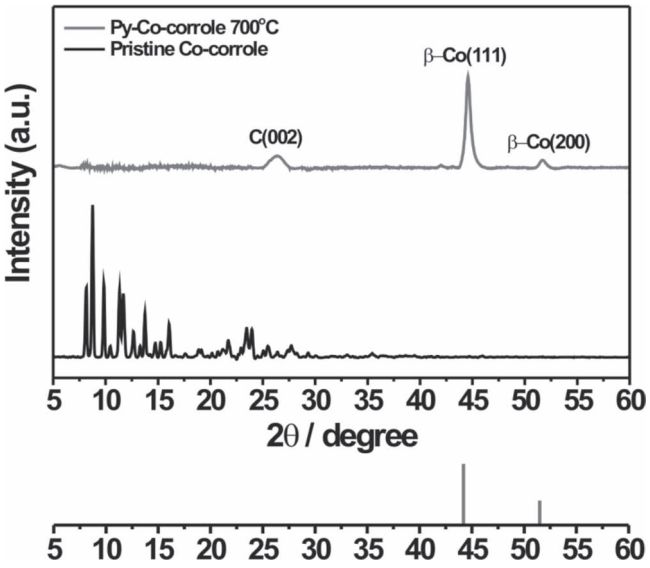

Figure 3. XRD patterns of pyrolyzed Co-corrole and pristine Co-corrole. The reference pattern of *β*-Co (JCPDS, PDF# 150806) is shown below the figure.

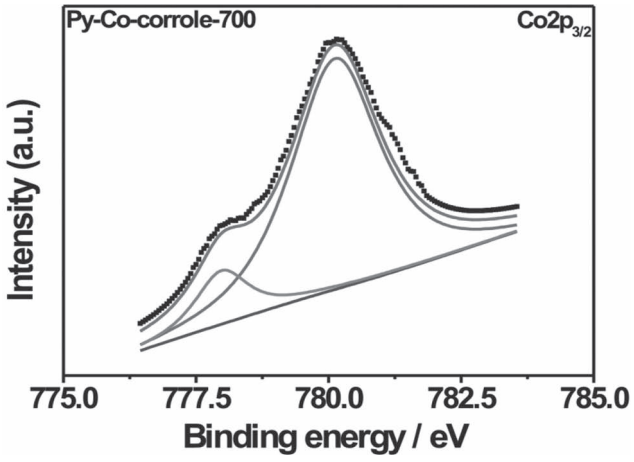

Figure 4. XPS showing the Co2p$_{3/2}$ spectrum of py-Co-corrole-700.

Pristine Co-corrole shows a peak at 398.7 eV, which is pyridinic-like nitrogen. After the pyrolysis, part of pyridinic-like nitrogen still exists, but the rest of carbon-nitrogen structure is converted into quaternary (graphitic)-type nitrogen, as shown at 401.4 eV. Chung et al. proposed that the quaternary-type nitrogen are expected to lower the carbon band gap energy and possibly promote catalytic activity.[15] Recently, some studies on nitrogen-doped carbon catalysts also reported that the graphitic (quaternary) nitrogen were found to have ORR catalytic activity.[16] It seems that nitrogen incorporation contributes the ORR enhancement. In the case of Co-corrole/C pyrolyzed at

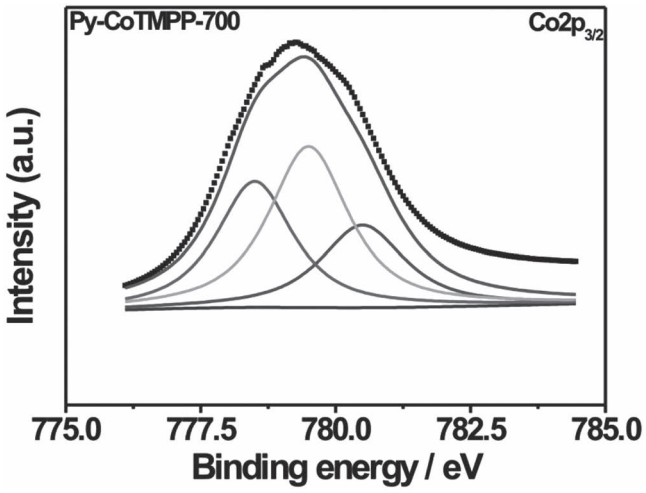

Figure 5. XPS showing the $Co2p_{3/2}$ spectrum of py-CoTMPP-700.

Table 1. The fitting results from the XPS $Co2p_{3/2}$ spectra of Figure 4 and 5.

Co $2p_{3/2}$	Possible structure		
	Co(0)	Co(II)O	Co(II)Nx
	(778.4 eV)	(779.4 eV)	(780.5 eV)
Py-Co-corrole-700	5.3%	–	94.7%
Py-CoTMPP-700	32.7%	23.6	43.7%

a desired high temperature, the central cobalt-containing corrole ring is partially destroyed, resulting in a new catalytic site which has much high ORR activity and stability. From Co2p and N1s of XPS spectra, the binding energies are changed by the pyrolysis, indicating that the interaction between cobalt and N_4-chelate changes the profile of adsorbed/desorbed energies of O_2, resulting in a favorable situation for the ORR activity.

The ORR behaviors of py-Co-corrole/C-700, py-CoTMPP/C and Co/C were determined using the RRDE approach. **Figure 7**a plots the current density and the ring current of py-Co-corrole/C-700, py-CoTMPP/C and Co/C. The typical ORR curve obtained in an acidic medium has three dominant regions of potential - the kinetic range (>0.8 V), the mixed range (0.8–0.6 V), and the mass-transfer range (<0.6 V). The disk current (I_d) curve of py-Co-corrole/C-700 is clearly higher than the py-CoTMPP/C or Co/C curve in all regions. The higher disk current shows that py-Co-corrole/C-700 has a much greater ORR activity. The nominal Co wt% of py-Co-corrole/C-700, py-CoTMPP/C and Co/C are 1.50%, 1.74% and 20%, respectively, although py-Co-corrole/C-700 has the lowest Co loading but the highest ORR activity. Figure 7b,c plot the n values and $\%H_2O_2$ in the ORR as functions of the potential of the GC disk, respectively. The observed n values of py-CoTMPP/C and Co/C are reduced to around 3.22 and 3.15, respectively, when a large over-potential of 0.2 V is applied. In py-Co-corrole/C-700, the n value and $\%H_2O_2$ are almost independent of the applied potential, which are calculated to be 3.85 and below 7.5%, respectively, revealing that the ORR over py-Co-corrole/C-700 proceeds mostly via the direct ORR pathway when a large range of over-potentials below 0.8 V were applied. **Figure 8** presents the recorded polarization plots of the PEFCs using py-Co-corrole/C-700 in the cathode, which generates a maximum power density of 275 mW cm^{-2}. Since Co-based catalysts have commonly shown less ORR activities than Fe-based catalysts form recent reviews,[6a,11a] the performance of py-Co-corrole/C-700 is less than the recent reports using Fe-based catalysts.[8,9] In order to compare the Co-based catalytic efficiency, **Table 3** shows the performances of Co-based catalysts reported in the papers. The 100-hour durability test of py-Co-corrole/C-700 as the cathode catalyst in the fuel cell by flowing H_2 and air fed into the anode and the cathode, respectively, is demonstrated in **Figure 9**. At 0.4 V, the cell current density remains nearly constant of 0.221 A cm^{-2} for the 100-hour operation.

The oxidation state of the transition metal, the redox potential of M(II)/M(III) and the ligand effect dominate the ORR activity of Fe-based and Co-based macrocyclic compounds.[17] According to investigations of Co-corrole, the central cobalt is formally in the Co(III) state.[12d,18] **Figure 10** plots the cyclic voltammetry curve of py-Co-corrole/C-700 in N_2-saturated 0.1 M $HClO_4$. It demonstrates that py-Co-corrole/C-700 does not exhibit well-defined redox peaks of Co(II)/Co(III) and Co(I)/Co(II). Since only 1.5 wt.% Co exists in the py-Co-corrole/C-700, the redox peak of Co(II)/

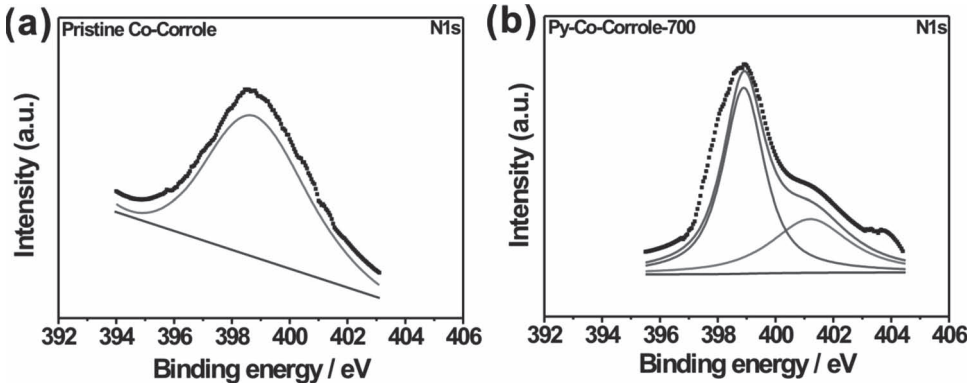

Figure 6. XPS showing the N1s spectra of a) prisitine Co-corrole and b) py-Co-corrole-700.

Table 2. The fitting results from the XPS N1s spectra of Figure 6.

N1s [atomic%]	Quaternary-type nitrogen (401.4 eV)	Pyridinic-like nitrogen (398.7 eV)
Pristine Co-corrole	–	100%
Py-C-corrole-700	36.4%	63.6%

Co(III) may be overwhelmed by the carbon-like capacitance. Additionally XANES results, plotted in **Figure 11**a, reveal that the Co cations oxidation states of pristine Co-corrole, py-Co-corrole-700, pristine CoTMPP, py-CoTMPP-700 and CoO powder are 3+, 2+, 2+, 2+ and 2+, respectively, revealing that pyrolysis changes the oxidation state after the pyrolysis. In a study of the mechanism of the ORR with an organic cobalt complex, Okada et al. identified four-, five- and six-coordinated Co(II)- or Co(III)-based compounds, of which the four-coordinated Co(II)-based compounds with a coplanar chelate structure exhibited the best catalytic performance.[19] Pristine Co-corrole is a five-coordinated species with Co(III), but after the pyrolysis, py-Co-corrole-700 is a four-coordinated Co(II) species. The magnified XANES results between 7700 and 7720 eV in Figure 11b indicate that the characteristic peak at about 7710 eV from CoO powder and pristine Co-corrole is strong; CoO and pristine Co-corrole are six-coordinated and five-coordinated species, respectively. However, the peak associated with py-Co-corrole-700 is shifted to a higher energy of 7713 eV has very low intensity. The six- and five-coordinated cobalamin (with M-N_4 structure of Co-corrin) reportedly yields the characteristic peaks at 7710 eV, but the four-coordinated cobalamin yields a characteristic peak at 7714 eV such as pristine CoTMPP,[20] revealing that the characteristic peak is at a higher energy when the M-N_4 species has a lower coordination number. These results support the claim that py-Co-corrole-700 is a four-coordinated species rather than a five-coordinated species. Since 94.7% content of py-Co-corrole-700 is four-coordinated Co(II)N_x compounds with a coplanar chelate structure, they may play the role of active sites for ORR.

The coordination kinetics of the adsorption of O_2 by the M-N_4 catalysts in the ORR is not fully understood.[11a] The four major available models of the adsorption of O_2 onto catalysts are Griffith's model, Pauling model, *trans*-Yeager model and *bridge*-Yeager model.[17b] Of these, the latter two predict four-electron transfer, and the *trans*-Yeager model is likely to be accurate on platinum catalysts but the *bridge*-Yeager model is likely to be accurate in cobalt macrocyclic compound.[12d,21] The cobalt-containing corrole ring with its corresponding coordination number is considered to participate in the ORR. When the cobalt-containing corrole ring is a four-coordinated species, the Co–PPh_3 bond is cleaved in the pyrolysis, causing the vacant site to coordinate easily with O_2. This hypothesis is supported by the study by Ramdhanie et al. of O_2 binding on a Co(II) corrole.[22] Collman et al. studied edge-plane graphite (EPG) disk electrodes that were modified with pre-adsorbed Co-corrole (Co-corrole/EPG), and they found that the ORR proceeds only at the Co-corrole structure with the central metal Co(II).[18a] When the central metal is Co(III), it is not expected to bind easily to O_2 and hence should not be catalytically active. The vitamin B12, which has a Co-corrin ring structure, can be compared in this respect because of its contracted ring structure. This

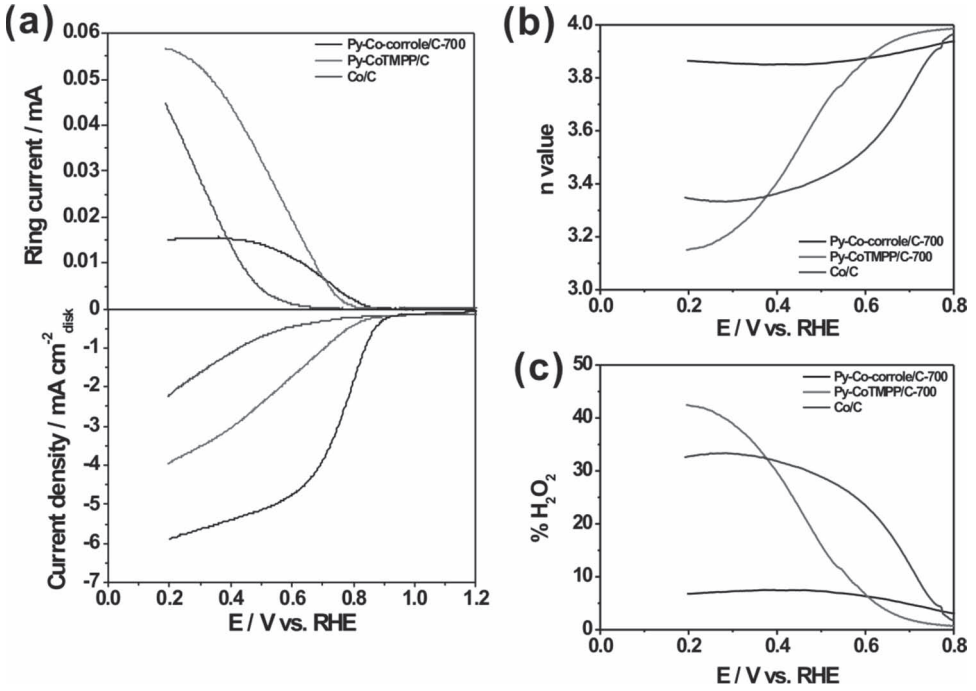

Figure 7. a) ORR curves for py-Co-corrole/C-700, py-CoTMPP/C, and Co/C; b) the n values; and c) %H_2O_2 of the catalysts dependence on disk potentials. Rotating speed: 1600 rpm; scan rate: 10 mV s^{-1}; ring potential: 1.2 V.

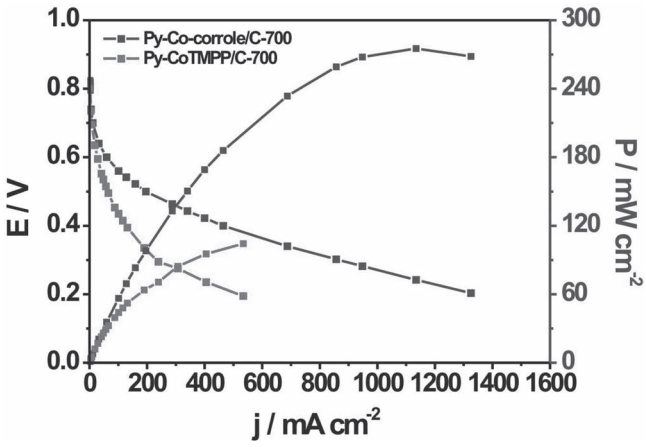

Figure 8. Polarization curve of the H_2-O_2 PEFC using py-Co-corrole/C-700 as the cathode. Operation temperature: 70 °C; back pressure of H_2 and O_2: 1 atm; anode catalyst: 0.25 mg cm^{-2} of Pt/C; cathode catalyst: 2.0 mg cm^{-2} of py-Co-corrole/C-700; electrolyte: Nafion 212 (H^+, DuPont).

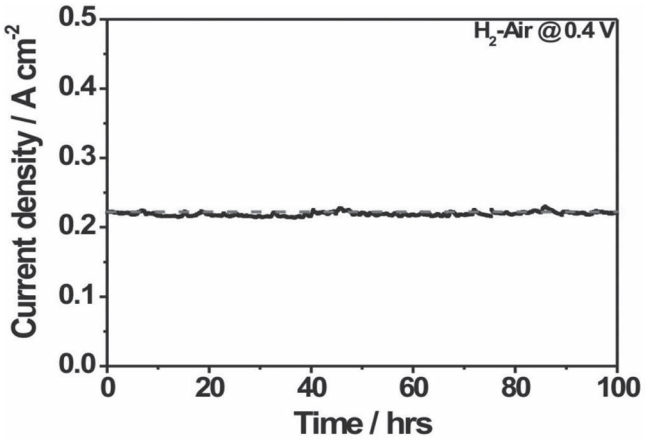

Figure 9. The 100-hour durability test of H_2-O_2 PEFC using py-Co-corrole/C-700. Operation conditions: H_2-Air, 70 °C and 1 atm of back pressure. Operation temperature: 70 °C; back pressure of H_2 and O_2: 1 atm; anode catalyst: 0.25 mg cm^{-2} of Pt/C; cathode catalyst: 2.0 mg cm^{-2} of py-Co-corrole/C-700; electrolyte: Nafion 212 (H^+, DuPont).

assumption is based on the study of Zagal et al., who utilized ordinary pyrolytic graphite electrodes that were modified with pre-adsorbed vitamin B12 (B12/OPG) in the ORR. This investigation revealed that with a central Co(II), B12/OPG is more active in undergoes a direct four-electron reduction pathway, while with a central Co(III), B12/OPG is more active in two-electron transfer.[23] However, no details of the coordination chemistry associated with enhanced ORR kinetics are available. The data, and with the hypothetical interpretations, herein potentially contribute to our understanding of the ORR mechanism of pyrolyzed Co-corrole in fuel-cell applications.

Table 3. The performances of Co-based catalysts reported previously.

Catalyst	Catalyst loading	Co loading	Test conditions	Maximum power density	Ref.
CoTMPP	12 mg cm^{-2}	350 μg cm^{-2}	H_2-O_2 PEFC 2 atm 50 °C	155 mW cm^{-2}	[2,26]
Co-PPY	N/A	60 μg cm^{-2}	H_2-O_2 PEFC 2 atm 80 °C	140 mW cm^{-2}	[2,7]
CoTMPP	4 mg cm^{-2}	N/A	H_2-O_2 PEFC 2 atm 80 °C	150 mW cm^{-2}	[2,27]
CoTPP	4 mg cm^{-2}	N/A	H_2-O_2 PEFC 2 atm 80 °C	150 mW cm^{-2}	[2,14b]
CoTMPP	N/A	80 μg cm^{-2}	H_2-O_2 PEFC 80 °C	90 mW cm^{-2}	[1,28]
Co-corrole	3 mg cm^{-2}	34 μg cm^{-2}	H_2-O_2 PEFC 1 atm 70 °C	275 mW cm^{-2}	This work

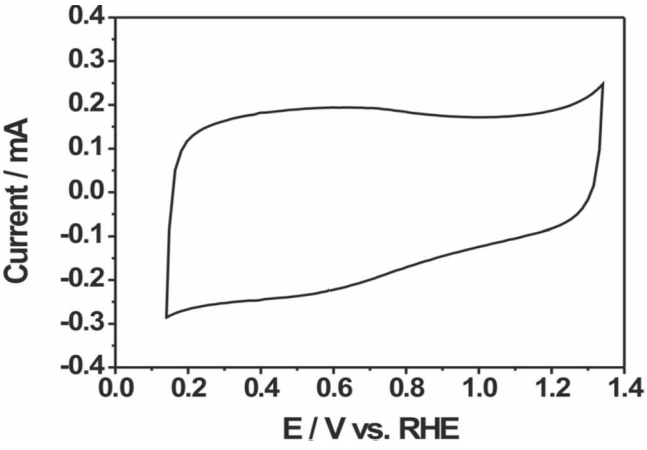

Figure 10. The cyclic voltammetry curve for py-Co-corrole/C-700 in N_2-purged 0.1 M $HClO_4$ solution.

3. Conclusions

Py-Co-corrole/C-700 demonstrates high potential activity in the ORR and favorable PEFC performance. The RRDE technique shows that py-Co-corrole/C-700 exhibits a preference for a direct four-electron reduction pathway. The H_2-O_2 PEFC uses py-Co-corrole/C-700 in the cathode, which shows higher performance but lower Co loading than previous studies in Co-based catalysts. The pyrolysis changes the coordination structure and oxidation state of Co-corrole, leading to the increase of ORR activity. The modifications of corrole structure with central metals and surrounding ligands have to be investigated furthermore.

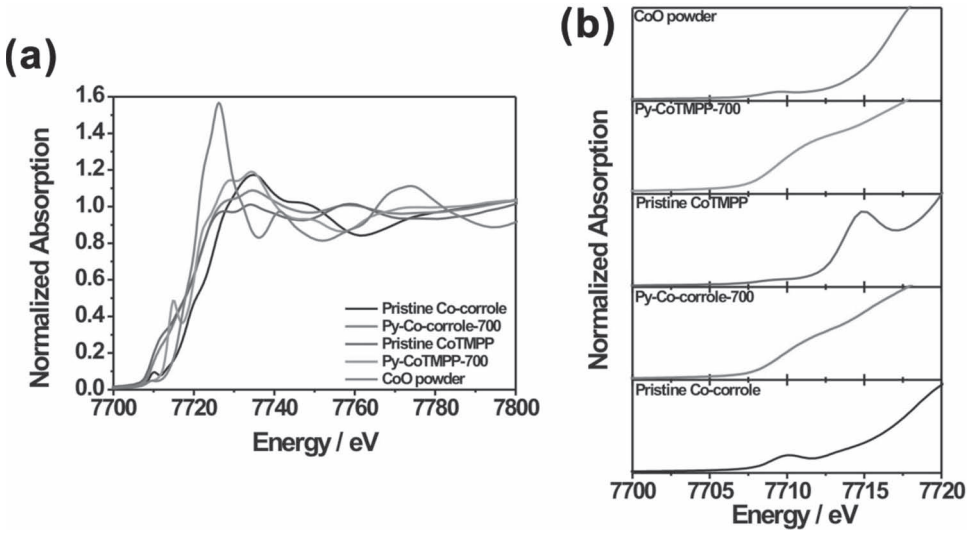

Figure 11. a) XANES spectra of pristine Co-corrole, py-Co-corrole-700, pristine CoTMPP, py-CoTMPP-700, and CoO powder. b) The expanded XANES spectra between 7700 and 7720 eV.

4. Experimental Section

Preparations of Pyrolyzed Co-Corrole and Pyrolyzed Co-Corrole/C: Co-corrole, (triphenylphosphine)(5,10,15-triphenylcorrolato)cobalt(III), was synthesized following modified version of a procedure in the literature.[24] The Supporting Information section presents details of the synthesis and characterizations of the compound. Scheme S1 presents the molecular structure of the as-prepared Co-corrole. The final catalyst was prepared according to the following procedure. Co-corrole (0.10 g) was dissolved in tetrahydrofuran (10 mL) with stirring for 30 min at room temperature. Then, carbon black (0.40 g, Vulcan XC-72R) was added to the Co-corrole solution, which was stirred for 30 min at room temperature. The mixture was heated using steam to 80 °C to eliminate the solvent. The suspension was filtered through filter paper to obtain the slurry, which was dried at room temperature under vacuum for 12 h.

Pyrolyzed Co-corrole supported by carbon black was prepared at various temperatures of 300, 500, 700, and 900 °C. The formed compounds were py-Co-corrole/C-300, py-Co-corrole/C-500, py-Co-corrole/C-700, and py-Co-corrole/C-900, respectively. In the common pyrolysis process, the slurry was loaded into a fused aluminum oxide boat, which was introduced into a furnace in a quartz tube; the specific temperature was increased at a rate of 20 °C per min in a nitrogen atmosphere, in which it remained for 2 h. Following the pyrolysis, the furnace was cooled to room temperature by natural convection. For example, at the pyrolyzed temperature of 700 °C, py-Co-corrole/C (0.42 g) demonstrated a total weight loss of about 16% throughout the process. To obtain X-ray diffraction patterns (XRD) and perform a thermogravimetric analysis (TGA) without overlap with the background associated with carbon black, the Co-corrole solution without added carbon black was loaded into a silica boat for pyrolysis, yielding py-Co-corrole.

Preparations of py-CoTMPP/C and Co/C: Pyrolyzed cobalt(II) tetramethoxyphenylporphyrin/C (py-CoTMPP/C) and Co/C were prepared to compare their electrochemical activities with those of py-Co-corrole. The py-CoTMPP/C was prepared as follows. Cobalt(II) tetramethoxyphenylporphyrin (0.10 g, CoTMPP, 99%, Aldrich) and carbon black (0.40 g, Vulcan XC-72R) were dispersed in *N,N*-dimethylmethanamide (DMF, 99.7%, Alfa Aesar) solution, which underwent 30 min of ultrasonication, to form a homogeneous solution. Thereafter, the solvent was removed by filtration and the mixed catalyst precipitate was collected on filter paper and dried in a vacuum at 60 °C for 24 h. Finally, the pyrolysis process was used to prepare py-CoTMPP/C at 600 °C. The mass of the as-prepared py-CoTMPP/C (0.425 g) represented a total weight loss of approximately 15.0% throughout the process. Similarly, in the preparation of Co/C, dried $CoCl_2$ (0.22 g) and carbon black (0.40 g, Vulcan XC-72R) were dispersed in de-ionized water and the above py-CoTMPP/C preparation process was implemented. In the final step, the catalyst mixture was pyrolyzed in a 5% hydrogen atmosphere 200 °C for 2 h.

Material Analysis: XRD was carried out using a Bruker D8 advanced diffractometer system with Cu $K\alpha_1$ radiation (λ = 1.54056 Å). TGA was carried outusing a thermal analysis instrument (TA Instrument Q500) at a scanning rate of 5 °C min^{-1} from room temperature up to 1000 °C, while the sample was kept in a constant flow of N_2. The X-ray photoelectron spectroscopy (XPS, VG ESCA Scientific Theta Probe using 1486.6 eV Al Kα source) was used to study the changes of $Co2p_{3/2}$ and N1s of pyrolyzed Co-corrole. The X-ray absorption near-edge structure (XANES) at the Co K-edge was recorded at beam line 17C1, which is based on a multi-pole wiggler source with a critical energy of 2.7 keV. The electron storage ring was operated at energy of 1.5 GeV with a beam current of 120–200 mA. The beam line employs a double Si(1 1 1)-crystal monochromator for energy selection with a resolution ($\Delta E/E$) of better than 2×10^{-4} in the energy range 5–15 keV. All spectra were obtained at room temperature in a transmission mode, and the intensities of incident and transmitted X-ray beams were measured using gas-filled ionization chambers. The catalyst powder was pressed into a slot of the stainless-steel holder and then placed in a cell for treatment under the desired conditions. The standard material, cobalt foil was measured simultaneously in the third ionization chamber to enable energy calibration scan by scan. The XANES data were processed, involving background subtraction, normalization with respect to the edge jump, Fourier transformation, and curve fitting, using computer programs that were implemented in the IFEFFIT software package. Additionally, the theoretical phase shifts and backscattering amplitudes for particular atom pairs were calculated using the FEFF7 code.[25]

Electrochemical Measurements: Electrochemical measurements were made in a three-compartment cell using a potentiostat/galvanostat instrument (Biologic Bi-stat). The working electrode was a rotating-ring disk electrode (RRDE, PINE AFE7R9GCPT) with a glassy carbon (GC) disk and a ring made of platinum. The counter electrode and reference electrode were Pt foil and a saturated calomel electrode (0.242 V vs. NHE), respectively. All potentials in this work are with reference to the reversible hydrogen electrode (RHE). The electrolyte in the ORR test was oxygen-saturated 0.1 M $HClO_4$ solution.

Catalyst ink was prepared by mixing catalyst (160 mg) with deionized water (20 mL). The ink (40 µL) and Nafion solution (5 µL, 0.1 wt.%) was dropped onto the GC disk, which was then left to dry in air at room temperature. Before the catalyst ink was deposited onto the GC disk, the GC disk had been polished to a mirror-like finish using 1.0 and then 0.05 µm alumina slurry. Cyclic voltammetry was performed on the catalysts at the specified scan rates. The ORR curves at the GC were plotted at a low scan rate of 10 mV s^{-1} to reduce the substantial non-Faradic current that would otherwise have been produced by the catalysts. To determine the yield of hydrogen peroxide in the ORR that was catalyzed by the catalysts on the GC disk, 1.2 V vs. RHE was applied to the ring to generate a current that oxidized the hydrogen peroxide.

Fuel Cell Test: A membrane-electrode-assembly (MEA) with an area of 5 cm^2 was made by hot-pressing two electrodes on both sides of a Nafion 212 (H^+, DuPont) at 135 °C and 130 kg cm^{-2} for 2 min. In the preparation of the specific cathode, py-Co-corrole/C was dispersed in a Nafion solution (5 wt.%) as a cathode catalyst ink, with catalysts to dry Nafion mass ratio of 1: 2. The cathode catalyst ink of py-Co-corrole/C (2.0 mg cm^{-2}) was hand-painted onto the carbon cloth, and the cathode was then dried at room temperature in a vacuum for 6 hours. The anode of MEA was a commercial electrode (E-TEK) - Pt/C (0.25 mg cm^{-2}). A polarization experiment was carried out on the PEFC at 70 °C, using hydrogen (0.1 slpm) and oxygen (0.15 slpm) through the anode and the cathode, respectively. Hydrogen and oxygen were passed through the humidifiers at 70 °C before they entered an MEA. The back pressure gauges on the anode and the cathode sides of on the sides of the anode and cathode were set to 1 atm. The PEFC performance was measured using a fuel-cell test station (Asia Pacific Fuel Cell Technologies, Ltd.) by recording the cell voltage and current after when they had reached steady values.

Supporting Information

Supporting Information is available from the Wiley Online Library or from the author.

Acknowledgements

H.-C.H and I.S. contributed equally to this work. The authors thank National Science Council (NSC 100-2218-E-011-013), Academia Sinica, and Ministry of Education (MOE Top University Projects - 100H451401) of Taiwan for financial support and experimental facility. The authors acknowledge the National Synchrotron Radiation Research Center, Hsinchu, Taiwan for X-ray absorption near-edge structure (Beam-line 17C1) analysis facility.

Received: January 28, 2012
Revised: March 21, 2012
Published online: May 8, 2012

[1] A. J. Appleby, *J. Electroanal. Chem.* **1993**, *357*, 117.
[2] R. Jasinski, *Nature* **1964**, *201*, 1212.
[3] a) N. A. Savastenko, V. Bruser, M. Bruser, K. Anklam, S. Kutschera, H. Steffen, A. Schmuhl, *J. Power Sources* **2007**, *165*, 24; b) P. Bogdanoff, I. Herrmann, M. Hilgendorff, I. Dorbandt, S. Fiechter, H. Tributsch, *J. New Mater. Electrochem. Syst.* **2004**, *7*, 85; c) C. Mocchil, S. Trasatti, *J. Mol. Catal. A: Chem.* **2003**, *204–205*, 713; d) X.-Y. Xie, Z.-F. Ma, X. Wu, Q.-Z. Ren, X. Yuan, Q.-Z. Jiang, L. Hu, *Electrochim. Acta* **2007**, *52*, 2091; e) H. Liu, C. Song, Y. Tang, J. Zhang, J. Zhang, *Electrochim. Acta* **2007**, *52*, 4532.
[4] a) W. Jingjie, T. Haolin, P. Mu, W. Zhaohui, M. Wentao, *Electrochim. Acta* **2009**, *54*, 1473; b) Y. Lu, R. G. Reddy, *Electrochim. Acta* **2007**, *52*, 2562.
[5] P. Convert, C. Coutanceau, P. Crouigneau, F. Gloaguen, C. Lamy, *J. Appl. Electrochem.* **2001**, *31*, 945.
[6] a) C. W. B. Bezerra, L. Zhang, K. Lee, H. Liu, A. L. B. Marques, E. P. Marques, H. Wang, J. Zhang, *Electrochim. Acta* **2008**, *53*, 4937; b) A. A. Serov, M. Min, G. Chai, S. Han, S. J. Seo, Y. Park, H. Kim, C. Kwak, *J. Appl. Electrochem.* **2009**, *39*, 1509; c) F. Jaouen, E. Proietti, M. Lefevre, R. Chenitz, J.-P. Dodelet, G. Wu, H. T. Chung, C. M. Johnston, P. Zelenay, *Energy Environ. Sci.* **2011**, *4*, 114.
[7] R. Bashyam, P. Zelenay, *Nature* **2006**, *443*, 63.
[8] M. Lefevre, E. Proietti, F. Jaouen, J.-P. Dodelet, *Science* **2009**, *324*, 71.
[9] G. Wu, K. L. More, C. M. Johnston, P. Zelenay, *Science* **2011**, *332*, 443.
[10] E. Proietti, F. Jaouen, M. Lefèvre, N. Larouche, J. Tian, J. Herranz, J.-P. Dodelet, *Nat. Commun.* **2011**, *2*, 416.
[11] a) Z. Chen, D. Higgins, A. Yu, L. Zhang, J. Zhang, *Energy Environ. Sci.* **2011**, *4*, 3167; b) A. Morozan, B. Jousselme, S. Palacin, *Energy Environ. Sci.* **2011**, *4*, 1238; c) D. S. Su, G. Sun, *Angew. Chem. Int. Ed.* **2011**, *50*, 11570; d) A. A. Gewirth, M. S. Thorum, *Inorg. Chem.* **2010**, *49*, 3557.
[12] a) Y. Gao, T. Akermark, J. Liu, L. Sun, B. Akermark, *J. Am. Chem. Soc.* **2009**, *131*, 8726; b) A. Okamoto, R. Nakamura, H. Osawa, K. Hashimoto, *J. Phys. Chem. C* **2008**, *112*, 19777; c) J. Grodkowski, P. Neta, E. Fujita, A. Mahammed, L. Simkhovich, Z. Gross, *J. Phys. Chem. A* **2002**, *106*, 4772; d) K. M. Kadish, L. Fremond, Z. Ou, J. Shao, C. Shi, F. C. Anson, F. Burdet, C. P. Gros, J.-M. Barbe, R. Guilard, *J. Am. Chem. Soc.* **2005**, *127*, 5625.
[13] a) C.-H. Wang, S.-T. Chang, H.-C. Hsu, H.-Y. Du, J. C.-S. Wu, L.-C. Chen, K.-H. Chen, *Diamond Relat. Mater.* **2011**, *20*, 322; b) G. Lalande, R. Cote, G. Tamizhmani, D. Guay, J. P. Dodelet, L. Dignard-Bailey, L. T. Weng, P. Bertrand, *Electrochim. Acta* **1995**, *40*, 2635.
[14] a) M. Manzoli, F. Boccuzzi, *J. Power Sources* **2005**, *145*, 161; b) S. Pylypenko, S. Mukherjee, T. S. Olson, P. Atanassov, *Electrochim. Acta* **2008**, *53*, 7875.
[15] H. T. Chung, C. M. Johnston, K. Artyushkova, M. Ferrandon, D. J. Myers, P. Zelenay, *Electrochem. Commun.* **2010**, *12*, 1792.
[16] a) K. Lee, L. Zhang, H. Lui, R. Hui, Z. Shi, J. Zhang, *Electrochim. Acta* **2009**, *54*, 4704; b) J.-i. Ozaki, N. Kimura, T. Anahara, A. Oya, *Carbon* **2007**, *45*, 1847.
[17] a) F. Beck, *J. Appl. Electrochem.* **1977**, *7*, 239; b) J. H. Zagal, *Coord. Chem. Rev.* **1992**, *119*, 89.
[18] a) J. P. Collman, M. Kaplun, R. A. Decreau, *Dalton Trans.* **2006**, 554; b) J.-M. Barbe, G. Canard, S. Brandes, R. Guilard, *Angew. Chem. Int. Ed.* **2005**, *44*, 3103.
[19] T. Okada, S. Gotou, M. Yoshida, M. Yuasa, T. Hirose, I. Sekine, *J. Inorg. Organomet. Polym.* **1999**, *9*, 199.
[20] E. M. Scheuring, W. Clavin, M. D. Wirt, L. M. Miller, R. F. Fischetti, Y. Lu, N. Mahoney, A. Xie, J.-j. Wu, M. R. Chance, *J. Phys. Chem.* **1996**, *100*, 3344.
[21] a) C. J. Chang, Z.-H. Loh, C. Shi, F. C. Anson, D. G. Nocera, *J. Am. Chem. Soc.* **2004**, *126*, 10013; b) E. Askarizadeh, S. B. Yaghoob, D. M. Boghaei, A. M. Z. Slawin, J. B. Love, *Chem. Commun. 46*, 710; c) S. Fukuzumi, K. Okamoto, Y. Tokuda, C. P. Gros, R. Guilard, *J. Am. Chem. Soc.* **2004**, *126*, 17059; d) S. Fukuzumi, K. Okamoto, C. P. Gros, R. Guilard, *J. Am. Chem. Soc.* **2004**, *126*, 10441;

e) G. Givaja, M. Volpe, M. A. Edwards, A. J. Blake, C. Wilson, M. Schröder, J. B. Love, *Angew. Chem. Int. Ed.* **2007**, *46*, 584.
[22] B. Ramdhanie, J. Telser, A. Caneschi, L. N. Zakharov, A. L. Rheingold, D. P. Goldberg, *J. Am. Chem. Soc.* **2004**, *126*, 2515.
[23] J. H. Zagal, M. J. Aguirre, M. A. Paez, *J. Electroanal. Chem.* **1997**, *437*, 45.
[24] a) B. Koszarna, D. T. Gryko, *J. Org. Chem.* **2006**, *71*, 3707; b) A. Mahammed, I. Giladi, I. Goldberg, Z. Gross, *Chemistry* **2001**, *7*, 4259.
[25] J. J. Rehr, R. C. Albers, S. I. Zabinsky, *Phys. Rev. Lett.* **1992**, *69*, 3397.
[26] Z.-F. Ma, X.-Y. Xie, X.-X. Ma, D.-Y. Zhang, Q. Ren, N. Heß-Mohr, V. M. Schmidt, *Electrochem. Commun.* **2006**, *8*, 389.
[27] T. S. Olson, K. Chapman, P. Atanassov, *J. Power Sources* **2008**, *183*, 557.
[28] F. Jaouen, J. Herranz, M. Lefevre, J.-P. Dodelet, U. I. Kramm, I. Herrmann, P. Bogdanoff, J. Maruyama, T. Nagaoka, A. Garsuch, J. R. Dahn, T. Olson, S. Pylypenko, P. Atanassov, E. A. Ustinov, *ACS Appl. Mater. Interfaces* **2009**, *1*, 1623.